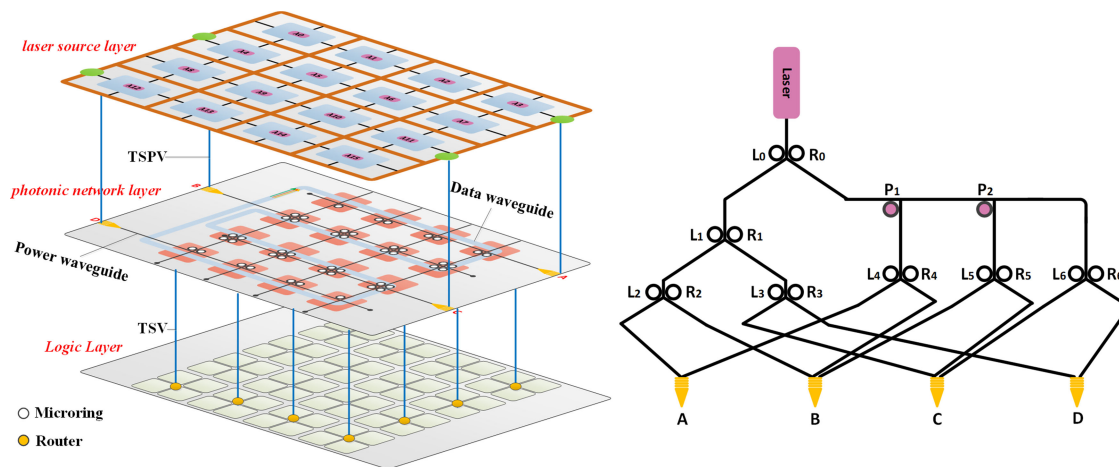


# A Group-Based Laser Power Supply Scheme for Photonic Network on Chip

Volume 11, Number 3, June 2019

Xiaolu Wang  
Huaxi Gu  
Yintang Yang  
Kun Wang



DOI: 10.1109/JPHOT.2019.2913676

1943-0655 © 2019 IEEE

# A Group-Based Laser Power Supply Scheme for Photonic Network on Chip

Xiaolu Wang, Huaxi Gu , Yintang Yang , and Kun Wang

State Key Laboratory of Integrated Service Networks and the Institute of Microelectronics,  
Xidian University, Xi'an 710126, China

DOI:10.1109/JPHOT.2019.2913676

1943-0655 © 2019 IEEE. Translations and content mining are permitted for academic research only.

Personal use is also permitted, but republication/redistribution requires IEEE permission.

See [http://www.ieee.org/publications\\_standards/publications/rights/index.html](http://www.ieee.org/publications_standards/publications/rights/index.html) for more information.

Manuscript received March 6, 2019; revised April 18, 2019; accepted April 24, 2019. Date of publication April 29, 2019; date of current version May 13, 2019. This work was supported by the National Science Foundation of China under Grants 61634004 and 61472300, the Fundamental Research Funds for the Central Universities Grant No. JB170107 and JB180309, china postdoctoral science foundation No. 2018M633465, and the key research and development plan of Shaanxi province No. 2017ZDCXL-GY-05-01. Corresponding author: Huaxi Gu (e-mail: hxgu@xidian.edu.cn).

**Abstract:** It is expected that the future multicore systems will significantly benefit from photonic interconnect technology because of its large bandwidth. However, the static power consumed by laser sources accounts for a large proportion of the overall power budget; thus, it has a negative impact on the performance of future photonic network on chip. In this paper, GLaP, a group-based static laser power supply approach is proposed. The communication backbone is investigated based on single-write-multiread crossbar. Generic laser power delivery and allocation architectures are proposed to match the bandwidths with the requirements of different nodes. The laser sources are shared across the network which enables significant reduction in laser power consumption. The evaluation results show that the laser power can be significantly saved compared with traditional laser supply schemes.

**Index Terms:** Photonic interconnect, Network-on-Chip, Laser Power Supply, Power Delivery, Power Allocation.

## 1. Introduction

High-Performance systems are facing a lot of challenges because of the growing energy costs dominated by data movement [1]. The silicon-photonic link technology is estimated to have one order of magnitude higher bandwidth density and much lower energy cost compared to the traditional electrical link technology [2]–[4]. The practical buffering technology is still a barrier. The bandwidth (in this paper, bandwidth represents the transmission rate) advantage of optical data transmission indicates a new approach to designing system-wide photonic on-chip networks. Many different silicon-photonic on-chip communication network architectures have been investigated. Although the silicon-photonic NoC provides larger bandwidth density and its link energy is data-dependent, a considerable amount of power is still dissipated in the laser source which is used for driving the silicon-photonic NoC [5]–[7].

There are generally two ways of providing laser power for on-chip communications. For the first one, the power supply network coincides with the communication network [2], i.e., the communication network uses the same waveguides with the power supply network. Fig. 1 shows the paradigm of the first laser power supply scheme based on wavelength-division multiplexed (WDM) photonic link. Light waves of wavelength  $\lambda_1$  and  $\lambda_2$  issued by a laser source are coupled into waveguides. The light waves pass a series of microring modulators, which are controlled by modulator drivers

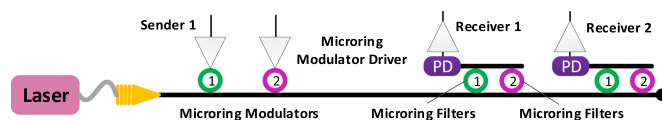


Fig. 1. WDM-based photonic link.

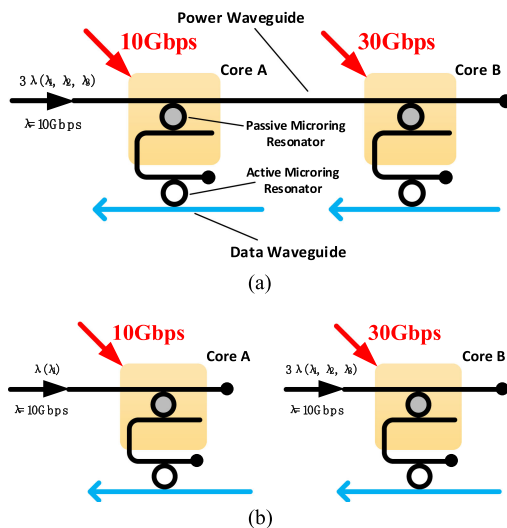


Fig. 2. Laser power supply scheme. (a) Traditional laser power supply scheme. (b) Group-based laser power supply scheme.

based on the data to be transmitted on the photonic link. The electrical signals are converted to be optical signal by modulators. The modulated optical signals travelling along the waveguide may pass through many microring filters. As for the receiver, the ring filter absorbs the light wave having the same resonant wavelength with the filter onto a photodetector. The photodetector current is sensed by an electrical receiver, and the optical signals are converted back into electrical signals. The main drawback of this structure is that the receiver side will not know whether the passing optical signals are sent to it without being informed early. If sender 1 wants to communicate with receiver 2, receiver 1 will also couple some power to determine whether it is the destination node. This part of power can be considered as additional loss. Hence, notification information should be sent to the receiver before data transmission, so that the receiver side could switch on its microring filter in advance.

To improve the communication efficiency, this paper mainly investigates the second power supply approach, in which the power network and the communication network are separated [9], [10]. Specifically, a power waveguide goes through all nodes with a range of different wavelengths travelling in it. Each node can couple the same amount of laser power. One of the most important characteristics of microring resonator is that the proportion of optical power coupled to another waveguide is determined by the gap, which represents the distance between microring resonator and waveguide [11]. Passive microring resonators have a fixed resonant wavelength that requires no external control but is susceptible to temperature changes. Hence, by changing this gap, we can decide how much power can be coupled into the drop port. If there is data to be transmitted, the coupled light wave will be modulated to the data waveguide by tuning the active microring resonators. Fig. 2(a) shows a traditional paradigm of the laser power supply scheme based on separated power network. The active microring resonator in each core can couple all different wavelengths in the power waveguide. Besides, the filters at the receiver side can be passive microring resonators.

In many cases, different cores have different data generation rates. This leads to the issue that different cores may need different bandwidths. Suppose the data generation rate of core A is

10 Gbps, the data generation rate of core B is 30 Gbps, and the modulation rate of each wavelength is 10 Gbps. In this global power supply scheme, the wavelengths injected into the power waveguide are shared by two cores. It is obvious that the required bandwidth is determined by the core with larger injection rate. Hence, the bandwidth provided should be 30 Gbps, and 3 different wavelengths should be multiplexed in the power waveguide. The 30 Gbps bandwidth is exactly appropriate for core B. However, it is superabundant for core A. Core A can only utilize 1/3 of the total bandwidth, namely, 1/3 of its time is occupied by data transmission and the rest 2/3 time is in idleness. Correspondingly, a large amount of laser power is not utilized. In this paper, we will employ a group-based static laser power supply scheme which is named GLaP which is proposed for fixed traffic pattern. The network is partitioned into multiple groups and each group is assigned with an individual power waveguide. The number of wavelengths injected into each power waveguide is determined by the bandwidth requirement of each group. Fig. 2(b) shows a paradigm of this group-based scheme, in which each group contains only one core. The data generation rate of core A is 10 Gbps, thus it is provided with only one wavelength  $\lambda_1$ . The data generation rate of core B is 30 Gbps, thus it is provided with only three wavelengths  $\lambda_1$ ,  $\lambda_2$ , and  $\lambda_3$ . It should be noted that to control the total number of wavelengths used, all wavelengths should be able to be shared by different cores. For instance,  $\lambda_1$  can be shared by both core A and core B. Hence, how to allocate wavelength to different cores will be an importance problem, which we will discuss in detail in Section 4.

In this paper, we make the following novel contributions: Proposing a new power supply scheme named GLaP. We focus on two parts in GLaP, i.e., power delivery architecture and power allocation architecture. The power delivery architecture is used to deliver optical power to all nodes, which is direct power source of all communications. The power allocation architecture is used to allocate laser power to different power waveguides of the delivery architecture. The rest of the paper is organized as follows. Section 2 introduces the related work, followed by the network architecture described in Section 3. In Section 4, we describe the power delivery architecture of GLaP, and then we show the power allocation architecture of GLaP. 3D integration and the case study of configuration is demonstrated in Section 5. The simulation analysis is illustrated in Section 6.

## 2. Related Work

The laser power consumption can never be ignored because it could negate the advantage of bandwidth density and the property of data-dependent energy consumption of the silicon-photonics links. To use silicon-photonics link technology for data communications in future high-performance systems, there is a need to come up with new approaches to reduce the power dissipated by the laser sources. The ultimate goal of laser power management is to guarantee the network performance, while reducing the power consumed in the laser sources at the same time.

A silicon-photonics NoC architecture based on multiple buses between private L1 caches and distributed L2 cache banks is proposed in [2]. It adopts a weighted time-division multiplexing (TDM) technique to allocate the laser power to different buses by switching on/off laser sources at runtime when the bandwidth requirement of an application varies, and the power consumption of laser sources is thus reduced. This design by switching on/off laser sources has the problem of delays in communication. Reference [12] proposes a prediction-based optical bandwidth scaling scheme (PROBE), which employs the information of former link utilization. The channel bandwidths are adjusted according to the network traffic to guarantee the communication performance by turning on/off proportions of the network, and thus reduce the static laser power. One of the biggest problems with the PROBE architecture is the number of laser sources required is proportional to the number of tiles in the network, and the design of the multi-layer binary tree waveguide requires a large number of waveguides. Although the power consumption can be reduced to some extent, the scalability is relatively poor. And a large number of optical splitters are used in the bandwidth allocation process, resulting in a large amount of loss [29]. Reference [13] also proposes a mechanism of controlling laser power consumption which switches on/off laser sources during periods requiring high/low bandwidth. However, switching the laser source on/off will increase

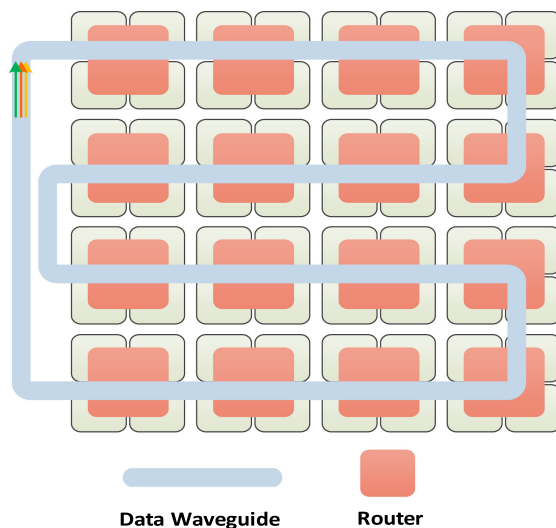


Fig. 3. Layout of 16-node network architecture.

network delay. Reference [14] introduces power topologies which consist of various power mode to reduce the overall interconnect power based on on-chip laser source. The more frequently communicating nodes use modes that consume less power, while less frequently communicating nodes use modes that consume more power. As far as the current technology is concerned, there are still some difficulties in implementation [21]. Reference [15] reduces the laser power dissipation dynamically by turning on and off the photonic links in the network when the corresponding L2 cache banks are active and inactive. Reference [16] presents an interconnect architecture which integrates clockwise and counter-clockwise nanophotonic crossbars. It improves the utilization of the static laser power, which is often squandered due to the insertion losses and unexploited bandwidth. This architecture requires longer waveguides, and the number of required microrings is higher than other designs, which consumes large on-chip resources. Reference [17] partitions computation and communication resources of the chip, and maximizes reuse across partitions by powered off laser sources that are not used during a certain period.

### 3. Network Architecture

This paper utilizes photonic Single-Write-Multi-Read crossbar (SWMR) to implement the on-chip interconnect network. Fig. 3 shows the layout of a 16-node network. Each node mainly consists of processing core and transmission/receiving module. The wavelengths are multiplexed in the data waveguides. Only one direction communication is allowed in the crossbar. The data waveguides go through every node in a serpentine way.

SWMR (Single-Write-Multi-Read) crossbar is a common candidate for high performance interconnect [5]. Fig. 4 shows the structure of an optical SWMR crossbar. The waveguides are classified into three types according to its functions, i.e., power waveguide, data waveguides ( $DW_0, DW_1, \dots, DW_{n-1}$ ) and reservation waveguides ( $RW_0, RW_1, \dots, RW_{n-1}$ ). For the purpose of convenience, the data and reservation waveguides are shown as lines in Fig. 3, and omitted the rings. Each node is assigned with an exclusive data waveguide to transmit information to all other nodes. A range of different wavelengths are injected into the power waveguide through the coupler. Each node is assigned with an array of passive broadband microring close to the power waveguide to couple a fraction of laser power to its local node. The gaps between these passive broadband microring resonators and the power waveguide are precisely configured in advance, which guarantees that the amount of power coupled by all passive microring resonators are exactly the same.

When there is transmission requirement for a certain node, the state of its active microring resonator against the data waveguide will be electrically controlled to modulate the laser power.

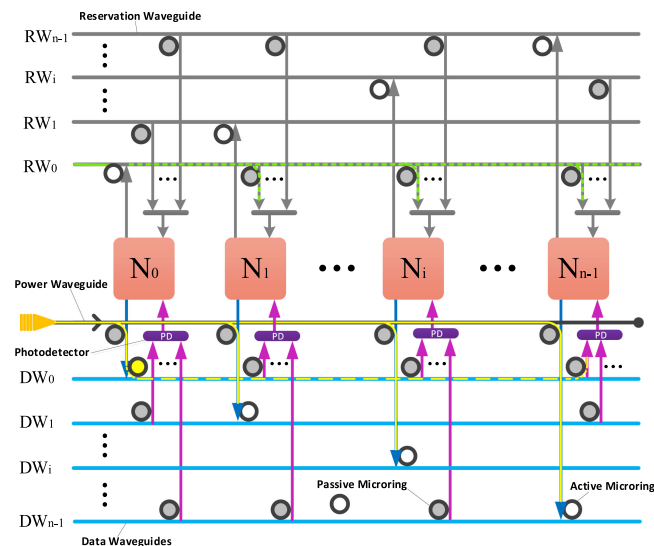


Fig. 4. SWMR crossbar structure.

The SWMR architecture requires optical reservation channels to notify the destination nodes in advance. The optical reservation waveguides are symmetric with the data waveguides, and are used to transmit small packets. For example, if node  $N_0$  wants to communicate with node  $N_{n-1}$ ,  $N_0$  will first modulate the light wave in  $RW_0$ , and the encoded optical data carrying the information of the destination address will be first broadcast to all other nodes.  $N_1, N_2, \dots, N_{n-1}$  will decide whether they are the destination node after receiving the data.  $N_{n-1}$  will know that it is the destination node of  $N_0$ , and will open the active microring of  $N_{n-1}$  on  $W_0$ , making it in resonance state while the microring resonators on  $DW_1, DW_2, \dots, DW_{n-2}$  of nodes  $N_1, N_2, \dots, N_{n-2}$  remain off.  $N_0$  can write data to  $DW_1$ , and  $N_{n-1}$  will couple the corresponding light packets into the light detection. And converting the optical signal into an electrical signal and receiving it into the local node.

#### 4. Laser Power Delivery Architecture

In this paper, the network architecture and laser power supply architecture are designed separately. The power waveguides are organized in a grid shape and covered the whole network. By configuring the power architecture, the whole network can be partitioned into several groups. The laser power delivery architecture of a 16-node network is shown as an example in Fig. 5. A, B, C, D are optical couplers. Different wavelengths are injected into the network via these couplers. The active broadband microring resonators are located on the intersections of the power waveguides. The microring resonators will be electrically configured to be two different states: on and off. If a broadband microring resonator is in on state, all of the passing wavelengths will be coupled into another waveguide. If a broadband microring resonator is in off state, all of the passing wavelengths will just go straight along the original waveguide. By changing the states of the microring resonators, the power delivery architecture can be configured to be different modes.

Fig. 6 shows different power modes of a 16-node network. The choice of specific power mode is based on the traffic distribution of the network, or in particular, the injection rates of all nodes. The bandwidth requirement of each group is determined by the node with maximum injection rate within the group. Obviously, different groups can be assigned with different bandwidths. Further, different configurations of power mode will also lead different laser power consumption. According

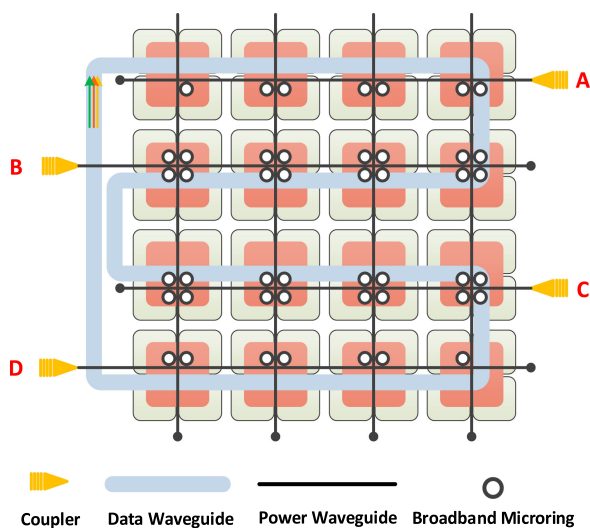


Fig. 5. Laser power delivery architecture of 16-node network.

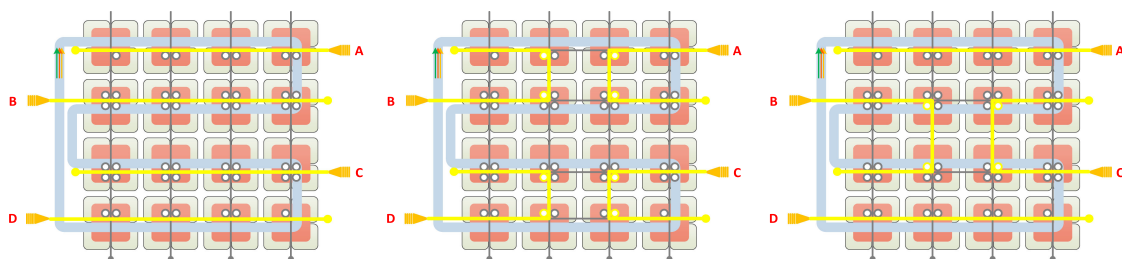


Fig. 6. Different power delivery modes.

to the specific network traffic distribution, the power delivery architecture will surely be configured to be the mode which can save the most laser power.

## 5. Laser Power Allocation Architecture

It is mentioned in the Section 3 that different groups may need different bandwidths under realistic circumstances. Hence, special architecture should be designed to achieve the allocation of laser power. Suppose the modulation rate of different wavelengths are the same, the total bandwidth allocated to a group should be

$$B = Wl\_Num \times Modu\_Rate \quad (1)$$

which is the product of the number of allocated wavelengths and the modulation rate of each wavelength. Therefore, the number of wavelengths and the bandwidth are linear related with each other. Suppose that each laser source issues only one wavelength, and the network is divided into  $n$  groups. The output power of each laser source should have  $n$  levels. Further, a delicate power allocation structure is needed to assign the laser power to any 1, 2, 3, ...,  $n$  groups of the network.

The network composed of 4 groups is taken as an example, which is shown in Fig. 5. For a laser source which issues wavelength  $\lambda$ , its output power of this wavelength can be adjusted to be four levels, which are  $p$ ,  $2p$ ,  $3p$  and  $4p$ . If each group has 4 nodes,  $p$  should satisfy the power requirement of all 4 nodes in a group, thus  $2p$  will satisfy the power requirement of all 8 nodes in two groups, and so forth. The purpose is design architectures to assign the laser power to any 1,

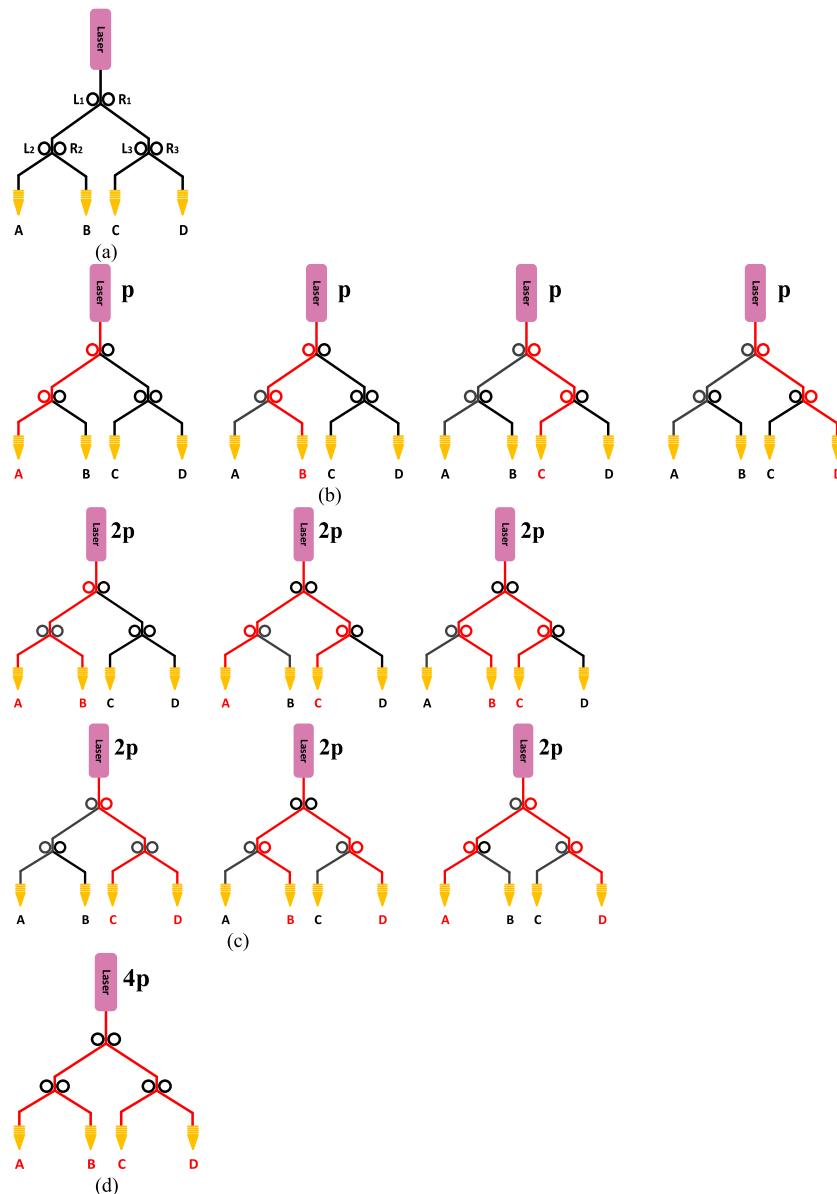


Fig. 7. Power allocation using architecture PX. (a) Power allocation architecture PX. (b) Allocate power to any group among 4 groups. (c) Allocate power to any 2 groups among 4 groups. (d) Allocate power to any 4 groups among 4 groups.

2, 3, 4 groups of the network. We solve this problem by considering two situations, and particularly design two architectures PX and PY.

Architecture PX, which is shown as Fig. 7(a), is used for allocating power to any 1, 2 or 4 groups when the output laser power is  $p$ ,  $2p$  or  $4p$ . The architecture has three pairs of active microring resonators. The power allocation is achieved by tuning the states of the microring resonators. By only tuning the right or left microring of each microring pair, the whole laser power will be directed to the left or right branch. By not activating any one of the microring pair, the laser power can be split into two equal parts [18]. Fig. 7(b) shows how to direct the power to group A, B, C or D when the output laser power is  $p$ . Fig. 7(c) how to equivalently divide the power to any two groups among A, B, C and D when the output laser power is  $2p$ . Fig. 7(d) shows that when the output laser power

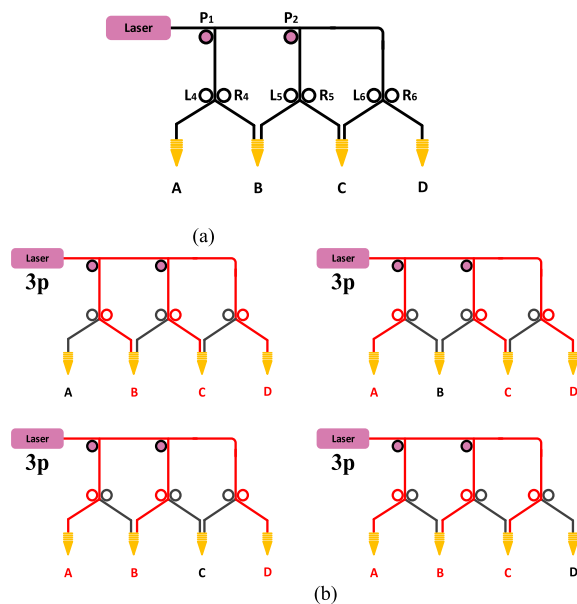


Fig. 8. Power allocation using architecture PY. (a) Power allocation architecture PY. (b) Allocate power to any 3 groups among 4 groups.

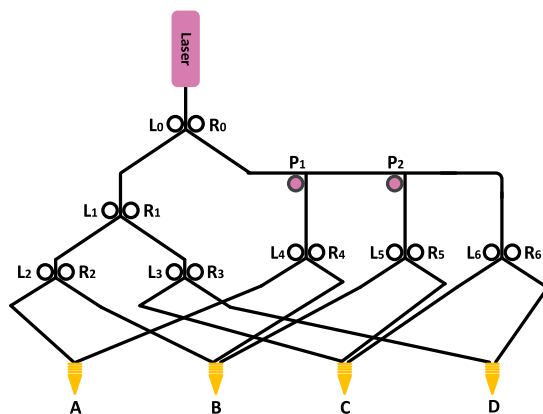


Fig. 9. Combination of PX and PY.

is  $4p$  and none of the microrings are activated, the optical laser power will be divided into two equal parts at every branch, thus all groups are allocated with the same optical power.

Architecture PY, which is shown as Fig. 8(a), is used for allocating power to any 3 groups when the output laser power is  $3p$ . Two passive microring resonators  $P_1$  and  $P_2$  are properly placed near the waveguide, so that the output laser power can be divided into three equal parts. The equally divided optical power will further be guided by the active microring pairs. Fig. 7 shows how to allocate  $3p$  laser power to any possible 3 groups among group A, B, C, and D.

As it is shown in Fig. 9, by combining the power allocation architectures PX and PY, we can get a compound architecture which can allocate laser power to any possible 1, 2, 3 or 4 groups among group A, B, C, and D. The active microring resonators  $L_0$  and  $R_0$  are used to select PX or PY. If  $L_0$  is switched on while  $R_0$  is switched off, the laser power will be directed to the left part and PX is used. If  $L_0$  is switched off while  $R_0$  is switched on, the laser power will be directed to the right part and PY is used.

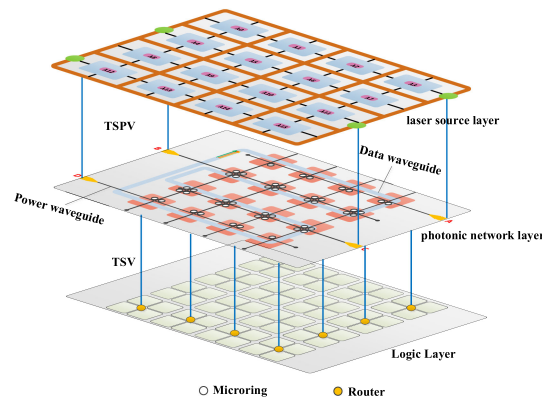


Fig. 10. Illustration of 3D stacked system of GLaP.

## 6. System Integration and Configuration

Commercial network-on-chip has not yet generally adopted silicon-photonic link technology, because the power dissipated by laser sources and thermal management of the photonic links could be significant and could even offset the advantage of communication capacity. Besides, packaging a large number of off-chip laser sources to drive the photonic NoC is quite technologically difficult and will introduce high link losses. A comb laser is generally adopted as an off-chip source, because packaging many single longitudinal-mode DFB lasers costs a lot. The coupling from an off-chip laser to a single-mode fiber will introduce around 2dB loss, and the coupling from the fiber to the silicon chip will introduce around 2dB loss when vertical grating couplers are employed [19]. The wall-plug efficiencies of comb lasers can be up to 30% [20]. However, when taking the losses into account, the realistic efficiencies of off-chip laser sources will descend to around 6%.

On-chip laser sources can be considered as potential candidates to drive the photonic NoC which decrease coupling losses and simplify packaging complexity, although they are not quite technologically mature [21]. It is reported that the loss of on-chip hybrid silicon lasers is around 0.5 dB [22], and the wall-plug efficiencies can be up to 15% [23], which usually outperform the off-chip laser sources. With a typical laser pitch of 125  $\mu\text{m}$  to 250  $\mu\text{m}$ , 100 to 200 laser sources per chip side is allowed [19], which is adequate for most of the state-of-the-art NoCs. To manage the wavelengths individually, each laser source emits a single wavelength and its output power can be adjusted [18].

We consider a 3D stacked system that consists of three individual layers in Fig. 10. The processor layer is fabricated using standard bulk CMOS process. The photonic network layer is next to the metal stack. Vertical metal vias are used to connect the processor layer and photonic network layer. The architecture of each core in the processor layer is similar to an IA-32 core used in the Intel Single-Chip Cloud Computer [4]. Placing laser sources in a top layer will minimize the influence of the temperature fluctuation of the bottom processor layer to the laser layer [21]. The interconnection of the laser source layer and the photonic network layer is achieved by TSPVs [24], [25]. The connection between the logic layer and the optical network layer is an electrical signal, and the electrical signal performs O/E, E/O conversion at the optical network layer. For example, in a 64-core system, every four cores constitute a cluster for the purpose of traffic convergence, and the data to or from each cluster is forwarded by its own router.

The configuration of the power architecture of the 64-core system is illustrated in Fig. 11. First, by monitoring the data generation rates of all nodes, the power mode which uses the least number of wavelengths will be adopted. Suppose group A needs 3 wavelengths, group B and C both need 1 wavelength, and group D needs 2 wavelengths. Wavelengths can be reused, thus group A can use  $\lambda_0, \lambda_1, \lambda_2$ ; group B and C can both use  $\lambda_0$ ; group D can use  $\lambda_0, \lambda_1$ . Correspondingly,  $\lambda_0$  will be shared by A, B, C;  $\lambda_1$  will be shared by A, C, D;  $\lambda_2$  will be used only by A. Fig. (a) shows the

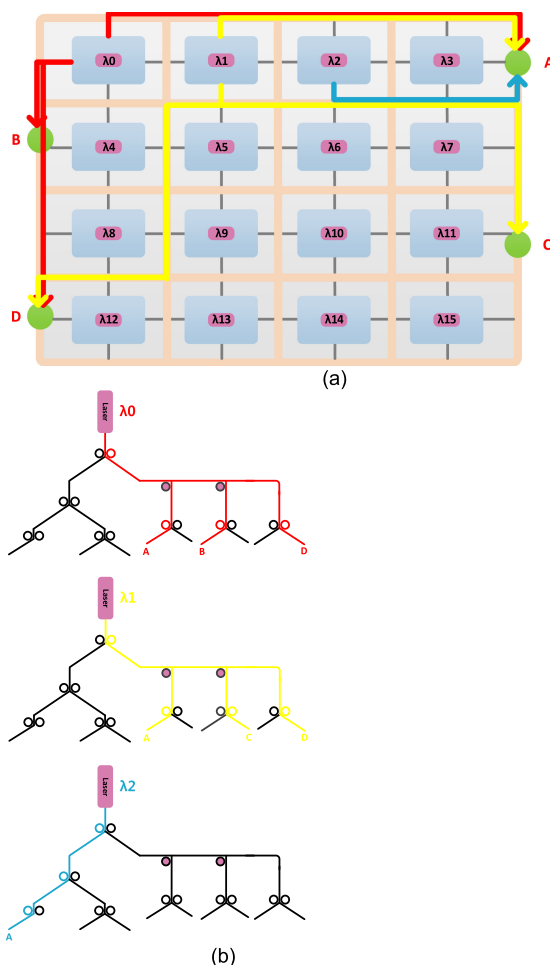


Fig. 11. Power allocation process. (a) Bandwidth requirement of each group. (b) Direct wavelengths to specific groups.

layout of the laser sources, the power allocation architectures which surround the laser sources, and the extended waveguides which are gathered to be a grid. Fig. (b) shows how the light waves of different wavelengths are directed to different groups by the power allocation architectures.

## 7. Evaluation

We evaluate the laser power consumption of 16-node, 36-node and 64-core NoCs. The communication backbones are implemented by photonic SWMR. For a certain wavelength, its expected laser power to guarantee the communication bandwidth of any node is supposed to be  $P$ , which represents the minimum power unit of a laser source.  $P$  can be determined by the following formula (1), where  $P_{sens}$  is the sensitivity of the photodetector, and  $L_{path}$  (dB) is the worst-case loss of the path from laser source to a certain destination node.

$$P = L_{path} - P_{sens} \quad (2)$$

The worst-case losses of different network architectures are considered, so that the provided laser power can guarantee even furthest communications. It can be directly calculated by formula (2), where  $Len_{sw}$  is the length of the straight waveguide,  $N_{TSPV}$  is the number of TSPV, and more information about the parameters are shown in Table 1 [26], [27]. It is estimated that based on 22 nm technology, the chip area of an  $8 \times 8$  grid of processor cores is around  $100 \text{ mm}^2$  [28]. Hence, the

TABLE 1  
Loss Parameters

Parameters	Meanings	Values
$L_{MRdrop}$	Drop loss per microring in on state	0.5dB
$L_{MRpass}$	Passing loss per microring in off state	0.005dB
$L_{TSPV}$	TSPV loss	1dB
$L_{prop}$	Waveguide propagation loss	0.274 dB/cm
$L_{bend}$	Waveguide bending loss	0.005dB
$L_{cross}$	Waveguide crossing loss	0.04dB
$P_{sens}$	Photodetector sensitivity	-14.2dBm

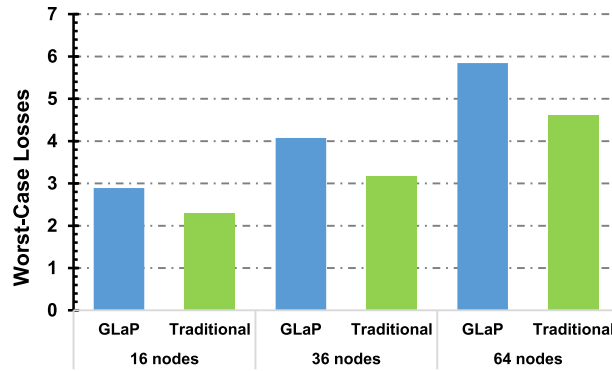


Fig. 12. Worst-case insertion losses.

side length of the chip is around 10mm, and the maximum length of straight waveguide is estimated to be 100 mm. Similarly, the maximum lengths of straight waveguide of a  $6 \times 6$  and  $4 \times 4$  grid of processor cores are estimated to be 52.5 mm and 25 mm.

$$L_{path} = Len_{SW} \times L_{prop} + \sum (L_{bend} + L_{cross} + L_{MRdrop} + L_{MRpass} + L_{TSPV}) \quad (3)$$

We compare the worst-case insertion losses of SWMRs based on GLaP and traditional power supply scheme, which are shown in Fig. 12. The losses introduced by all waveguides and microring resonators in the network and power supply architectures are considered. It can be seen that the worst-case losses of SWMR based on proposed GLaP is somewhat higher than SWMR based on traditional laser power supply scheme. This is because additional waveguide crossings and bends are introduced in GLaP.

The distribution of data generation rate for an  $N \times N$  network can be denoted by the following matrix:

$$\begin{bmatrix} r_{11} & \cdots & r_{1N} \\ \vdots & \ddots & \vdots \\ r_{N1} & \cdots & r_{NN} \end{bmatrix}$$

The data injection rate of the node in row  $i$  column  $j$  is  $r_{ij}$ . We assume that  $r_{ij}$  is a random value uniformly distributed between 0 to 100 Gbps. The modulation rate of each wavelength is assumed to be 10 Gbps. The packet length is set to be 1024bit. Each source node sends packets to all other nodes with the same probability. The laser power consumptions of different architectures using different power delivery mode are compared. Similar to the power delivery modes of  $4 \times 4$  network shown in Fig. 6, we employ three different power delivery mode I, II and III for generic

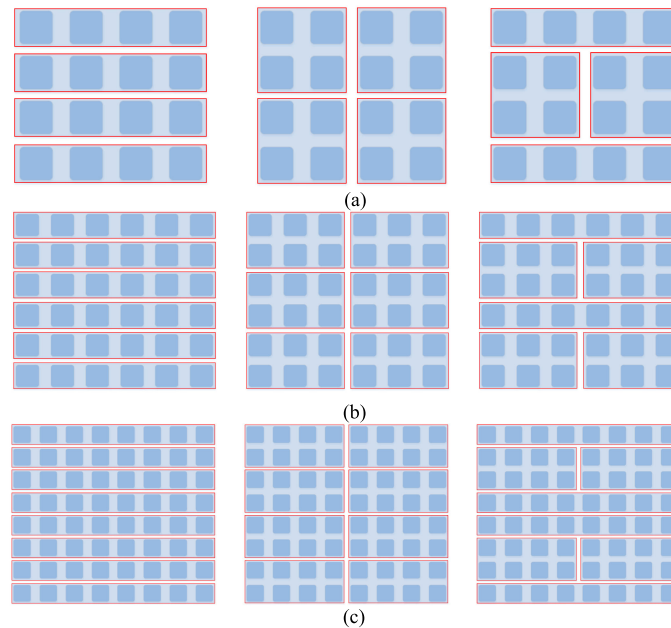


Fig. 13. Power delivery modes. (a) Three power delivery modes of 16-node network. (b) Three power modes delivery of 36-node network. (c) Three power delivery modes of 64-node network.

$N \times N$  network. For power delivery mode I, the network is divided into several rows, the first row  $r_{11}$  to  $r_{1N}$  forms a group which is assigned with a single power waveguide, the second row  $r_{21}$  to  $r_{2N}$  is another group, accordingly, the last group is formed by  $r_{N1}$  to  $r_{NN}$ . For power delivery mode II, the network is divided into several rectangular parts, i.e.,  $r_{11}, r_{12}, \dots, r_{1, N/2}, r_{21}, r_{22}, \dots, r_{2, N/2}$  are put in a group,  $r_{1, N/2+1}, r_{1, N/2+2}, \dots, r_{1N}, r_{2, N/2+1}, r_{2, N/2+2}, \dots, r_{2N}$  are put in another group, etc. For power delivery mode III, the row groups and rectangle groups exist alternately from up to down. Fig. 13 shows the specific power delivery modes of networks of 16-, 36-, and 64-node networks.

Fig. 14 shows the comparison of throughputs and normalized laser power consumptions of 16-, 36-, and 64-node SWMR crossbars. The curves in the figures show how throughputs varies with the increase of total provided bandwidths. The total provided bandwidth represents the sum of transmission bandwidth all nodes acquire, and throughput is the amount of data all nodes receive within a time unit. Theoretically, the higher the total bandwidth is provided, the shorter transmission delay will be, thus higher throughput can be achieved. When the total bandwidth exceeds a certain level, the throughput will no longer increase, which is referred to as saturation status. This is because the network is pushed to its limit, thus the overall data injection rate and the overall data receiving rate reach a balance. It is shown in Fig. 14(a), (b) and (c) that the SWMRs with the same number of nodes have the same saturation throughputs. Moreover, GLaP with different power delivery modes can reach the saturation point much earlier than the traditional one.

The provided bandwidth corresponds to specific overall laser power. Suppose that the minimum provided bandwidth of saturation status is  $B_S$ . To meet the transmission requirements of all nodes, the minimum saturation bandwidth corresponds to the minimum overall laser power. Since the modulation rates of each wavelength is 10 Gbps, the minimum overall laser power can be calculated as follows:

$$P_{laser} = P \times (B_S/10) \quad (4)$$

The bar charts in Fig. 14 shows that normalized minimum overall laser power consumptions of GLaP with different power delivery modes and traditional laser power supply scheme. SWMR crossbars using traditional power supply scheme are considered as baselines. Compared with the traditional scheme, 16-node SWMR using GLaP saves 17% to 31% laser power by using power

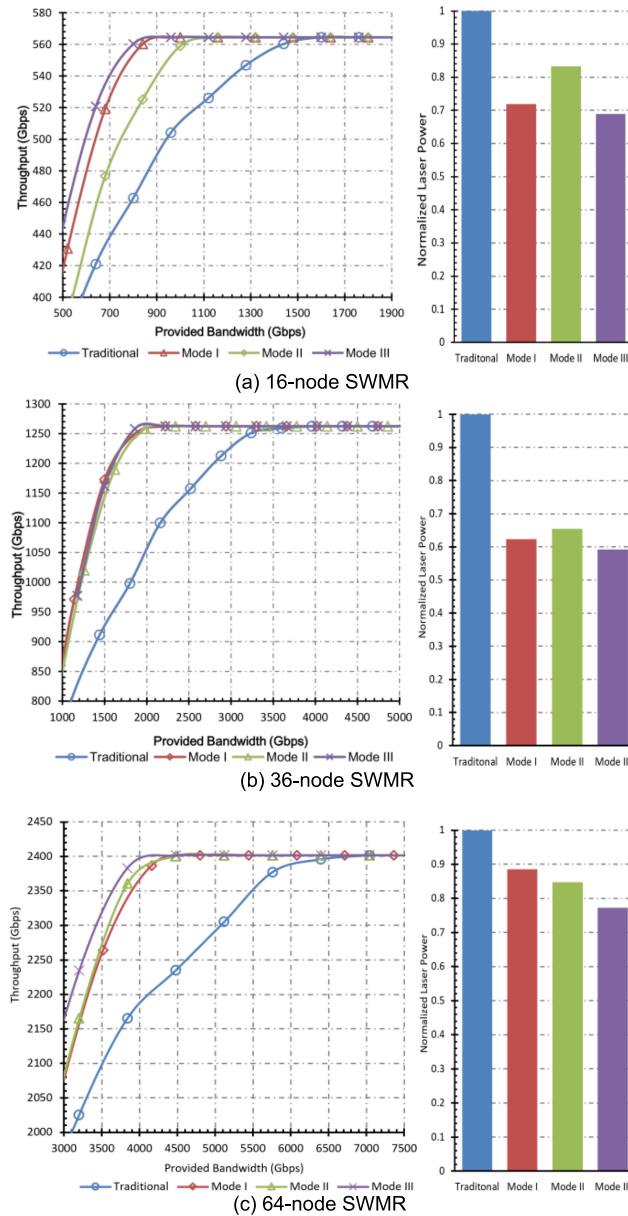


Fig. 14. Throughputs and normalized laser power consumptions.

delivery mode I, II or III. For 36-node SWMR, 35% to 41% laser power can be saved. For 64-node SWMR, 12% to 23% laser power can be saved. GLaP consumes prominently less laser power because the provided bandwidths match the realistic requirements within the network. It is also indicated that although the GLaP introduces more insertion loss, the extra laser power can still be significantly reduced by using more reasonable laser power delivery and allocation architectures.

## 8. Conclusion

In this paper, a laser power delivery and allocation scheme based on SWMR crossbar is proposed. Bandwidth requirements of different nodes within the network may vary a lot under realistic circumstances. In this regard, a laser power delivery and allocation architecture is proposed to provide bandwidths according to the requirements of different nodes. The provided bandwidth will guaran-

tee the communication performance of the network and approximate the actual data generation rate of different nodes. It is shown that the laser power consumptions witness a substantial reduction by using the proposed scheme.

## References

- [1] S. Rumley, D. Nikolova, R. Hendry, Q. Li, D. Calhoun, and K. Bergman, "Silicon photonics for exascale systems," *J. Lightw. Technol.*, vol. 33, no. 3, pp. 547–562, Feb. 2015.
- [2] C. Chen and A. Joshi, "Runtime management of laser power in silicon-photonics multibus NoC architecture," *IEEE J. Sel. Topics Quantum Electron.*, vol. 19, no. 2, Mar./Apr. 2013, Art. no. 3700713.
- [3] C. Batten *et al.*, "Building many-core processor-to-DRAM networks with monolithic CMOS silicon photonics," *IEEE Micro*, vol. 29, no. 4, pp. 8–21, 2009.
- [4] J. Howard *et al.*, "A 48-core IA-32 message-passing processor with DVFS in 45 nm CMOS," in *Proc. IEEE Int. Solid-State Circuits Conf. Dig. Technol. Papers*, Feb. 2010, pp. 108–109.
- [5] Y. Pan, P. Kumar, J. Kim, G. Memik, Y. Zhang, and A. Choudhary, "Firefly: Illuminating future network-on-chip with nanophotonics," in *Proc. 36th Annu. Int. Symp. Comput. Archit.*, 2009, pp. 429–440.
- [6] A. Joshi *et al.*, "Silicon-photonics networks for global on-chip communication," in *Proc. 3rd ACM/IEEE Int. Symp. Netw. Chip*, Washington, DC, USA, May 2009, pp. 124–133.
- [7] Y. Pan, J. Kim, and G. Memik, "Flexishare: Channel sharing for an energy-efficient nanophotonic crossbar," in *Proc. 16th Int. Symp. High-Perform. Comput. Archit.*, 2010, pp. 1–12.
- [8] H. Gu, K. Chen, Y. Yang, Z. Chen, and B. Zhang, "MRONoC: A low latency and energy efficient on chip optical interconnect architecture," *IEEE Photon. J.*, vol. 9, no. 1, Feb. 2017, Art. no. 4500412.
- [9] D. Vantrease *et al.*, "Corona: System implications of emerging nanophotonic technology," in *Proc. Int. Symp. Comput. Archit.*, vol. 36, 2008, no. 3, pp. 153–164.
- [10] Z. Wang, H. Gu, Y. Yang, and B. Zhang, "Power allocation method for TDM-based optical network on chip," *IEEE Photon. Technol. Lett.*, vol. 25, no. 10, pp. 973–976, May 2013.
- [11] Z. Su *et al.*, "An on-chip partial drop wavelength selective broadcast network," in *Proc. Conf. Lasers Electro-Opt. Sci. Innov.*, 2014, pp. 1–2.
- [12] L. Zhou and A. K. Kodi, "Probe: Prediction-based optical bandwidth scaling for energy-efficient NoCs," in *Proc. 7th IEEE/ACM Int. Symp. Netw. Chip*, 2013, pp. 1–8.
- [13] Y. Demir and N. Hardavellas, "Ecolaser: An adaptive laser control for energy-efficient on-chip photonic interconnects," in *Proc. ACM Int. Symp. Low Power Electron. Des.*, 2014, pp. 3–8.
- [14] J. Pang, C. Dwyer, and A. R. Lebeck, "More is less, less is more: Molecular-scale photonic NoC power topologies," in *Proc. 20th Int. Conf. Archit. Support Program. Lang. Operating Syst.*, 2015, pp. 283–296.
- [15] C. Chen, J. L. Abellán, and A. Joshi, "Managing laser power in silicon-photonics NoC through cache and NoC reconfiguration," *IEEE Trans. Comput.-Aided Des. Integr. Circuits Syst.*, vol. 34, no. 6, pp. 972–985, Jun. 2015.
- [16] M. Kennedy and A. K. Kodi, "Bandwidth adaptive nanophotonic crossbars with clockwise/counter-clockwise optical routing," in *Proc. 28th IEEE Int. Conf. VLSI Des.*, 2015, pp. 123–128.
- [17] M. Ortin *et al.*, "Partitioning strategies of wavelength-routed optical networks-on-chip for laser power minimization," in *Proc. IEEE Workshop Exploiting Silicon Photon. Energy-Efficient High Perform. Comput.*, 2015, pp. 17–24.
- [18] B. Neel, M. Kennedy, and A. Kodi, "Dynamic power reduction techniques in on-chip photonic interconnects," in *Proc. 25th Ed. Great Lakes Symp. VLSI*, 2015, pp. 249–252.
- [19] M. J. R. Heck and J. E. Bowers, "Energy efficient and energy proportional optical interconnects for multi-core processors: Driving the need for on-chip sources," *IEEE J. Sel. Topics Quantum Electron.*, vol. 20, no. 4, pp. 332–343, Jul./Aug. 2014.
- [20] J. Ahn *et al.*, "Devices and architectures for photonic chip-scale integration," *Appl. Phys. A*, vol. 95, no. 4, pp. 989–997, 2009.
- [21] C. Chen, T. Zhang, P. Contu, J. Klamkin, A. K. Coskun, and A. Joshi, "Sharing and placement of on-chip laser sources in silicon-photonics NoCs," in *Proc. 8th IEEE/ACM Int. Symp. Netw. Chip*, 2014, pp. 88–95.
- [22] G. Kurczveil, P. Pintus, M. J. R. Heck, J. D. Peters, and J. E. Bowers, "Characterization of insertion loss and back reflection in passive hybrid silicon tapers," *IEEE Photon. J.*, vol. 5, no. 2, Apr. 2013, Art. no. 6600410.
- [23] B. R. Koch *et al.*, "Integrated silicon photonic laser sources for telecom and datacom," in *Proc. Nat. Fiber Opt. Eng. Conf.*, Anaheim, CA, USA, Mar. 17–21, 2013, pp. 1–3.
- [24] A. Noriki, K. Lee, J. Bea, T. Fukushima, T. Tanaka, and M. Koyanagi, "Through-silicon photonic via and unidirectional coupler for high-speed data transmission in optoelectronic three-dimensional LSI," *IEEE Electron Device Lett.*, vol. 33, no. 2, pp. 221–223, Feb. 2012.
- [25] A. Noriki, K. Lee, J. Bea, T. Fukushima, T. Tanaka, and M. Koyanagi, "Through silicon photonic via (TSPV) with Si core for low loss and high-speed data transmission in opto-electronic 3-D LSI," in *Proc. IEEE Int. 3D Syst. Integr. Conf.*, 2010, pp. 1–4.
- [26] E. Fusella and A. Cilaro, "H<sup>2</sup>ONoC: A hybrid optical–electronic NoC based on hybrid topology," *IEEE Trans. Very Large Scale Integr. Syst.*, vol. 25, no. 1, pp. 330–343, 2017.
- [27] S. Werner, J. Navaridas, and M. Lujan, "Designing low-power, low-latency networks-on-chip by optimally combining electrical and optical links," in *Proc. IEEE Int. Symp. High Perform. Comput. Archit.*, 2017, pp. 265–276.
- [28] D. A. B. Miller, "Device requirements for optical interconnects to silicon chips," *Proc. IEEE*, vol. 97, no. 7, pp. 1166–1185, Jul. 2009.
- [29] Y. Urino *et al.*, "Demonstration of 12.5-Gbps optical interconnects integrated with lasers, optical splitters, optical modulators and photodetectors on a single silicon substrate," *Opt. Exp.*, vol. 20, no. 26, pp. B256–B263, 2012.